Overall Buckling Behavior of All-Steel Buckling Restrained Braces

Nader, Hoveidae
Ph.D. candidate in Sahand University of Technology, Tabriz, Iran and Researcher in Ecole Polytechnique de Montreal, QC. Canada

Behzad, Rafezy
Associate Professor, Civil Engineering Faculty, Sahand University of Technology, Sahand, Tabriz, East Azarbayjan, Iran

SUMMARY
One of the key requirements for the desirable mechanical behavior of buckling restrained braces (BRBs) under earthquake loading is to prevent global buckling until the brace member reaches sufficient plastic deformation and ductility. This paper presents finite element analysis results of proposed all-steel buckling restrained braces. The proposed BRBs have identical core sections but different buckling restraining mechanisms (BRMs). The objective of the analysis is to conduct a parametric study of BRBs with different amounts of gap (between the core and the BRM) and initial imperfections to investigate the global buckling behavior of the brace. The results of the analysis showed that BRM flexural stiffness could significantly affect the global buckling behavior of a brace, regardless of the size of the gap. In addition, a minimum ratio of the Euler buckling load of the restraining member to the yield strength of the core, P_e/P_y, is suggested for design purposes.

Keywords: *All-steel buckling restrained brace, Global buckling, Finite element analysis, Cyclic loading*

1. INTRODUCTION

Buckling restrained braced frames (BRBFs) for seismic load resistance have been widely used in recent years. A BRBF differs from a conventionally braced frame because it yields under both tension and compression without significant buckling. Most buckling restrained brace (BRB) members currently available are built by inserting a steel plate into a steel tube filled with mortar or concrete. The steel plate is restrained laterally by the mortar or the steel tube and can yield in compression as well as tension, which results in comparable yield resistance and ductility, as well as a stable hysteretic behavior in BRBs. The hysteretic curve of a BRB is stable, symmetrical, and ample (Black et al. 2002). Inoue et al. (2001) introduced buckling restrained braces as hysteretic dampers to enhance the seismic response of building structures. As shown in Fig. 1, a typical BRB member consists of a steel core, a buckling restraining mechanism (BRM), and a separation gap or unbonding agent, allowing independent axial deformation of the inner core relative to the BRM. Numerous researchers have conducted experiments and numerical analyses on BRBs for incorporation into seismic force resisting systems. Qiang (2005) investigated the use of BRBs for practical applications for buildings in Asia. Clark et al. (1999) suggested a design procedure for buildings incorporating BRBs. Black et al. (2002) performed component testing of BRBs and modeled a hysteretic curve to compare the test results. Sabelli et al. (2003) reported seismic demands on BRBs through a seismic response analysis of BRB frames, and Fahnestock et al. (2007) conducted a numerical analysis and pseudo dynamic experiments of large-scale BRB frames in the US.

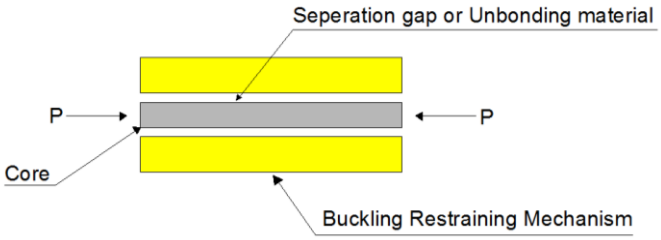

Figure 1. Components of a BRB [10]

The local buckling behavior of BRBs has been studied by Takeuchi et al. (2005). The effective buckling load of BRBs considering the stiffness of the end connection was recently studied by Tembata et al. (2004) and Kinoshita et al. (2007). Previous studies have demonstrated the potential of manufacturing BRB systems made entirely of steel, called all-steel BRBs (Tremblay at al. 2006). In a common all-steel BRB, the steel inner core is sandwiched between a buckling restraining mechanism made entirely of steel components, thus avoiding the costs of the mortar needed in conventional BRBs. This eliminates the fabrication steps associated with pouring and curing the mortar or concrete, significantly reducing manufacturing time and costs. In addition, such a BRB can be easily disassembled for inspection after an earthquake. Experimental and analytical studies on the deformation performance and dynamic response of BRBs have been performed by Kato (2002), Watanabe (2003), and Usami (2006). The restraining member proposed previously was a mortar-filled steel section, which made an extremely rigid member. In such types of BRBs, the brace member and the BRM were integrated, and overall buckling did not occur. However, in all-steel BRBs, which are considered to be a new generation of BRBs, the brace system is made completely of steel, and the BRM system is lighter in comparison with conventional BRBs, which leads to a high potential for brace overall buckling caused by the low rigidity and stiffness of the BRM. The hysteretic behavior of all-steel BRBs was experimentally investigated by Tremblay et al. (2006). An experimental study on the hysteretic behavior of all-steel BRBs was also conducted by Eryashar et al. (2010).

The following characteristics are considered necessary for the safe performance of BRBs: 1) the prevention of overall buckling, 2) the prevention of core local buckling, 3) the prevention of low cycle fatigue of the brace member, and 4) high strength of the joint parts and connections. In this paper, the first characteristic (i.e., overall buckling behavior) is examined further.

Assume a BRB member with initial deflection under compression. When the inner core with initial inherent imperfection deflects under compression, it comes into contact with the BRM, the contact forces increase the out-of-plane deformation of the entire BRB and strength deterioration occurs before the brace member reaches the target displacement if the rigidity and strength of the BRM are insufficient. According to the AISC 2005 guidelines for qualifying cyclic tests of BRBs (AISC2005), a BRB should sustain axial deformations up to $2\Delta_{\mathrm{bm}}$, where Δ_{bm} is the brace axial deformation corresponding to the design story drift. The buckling restraining mechanism should have enough strength and rigidity to prevent overall buckling of the brace during axial deformation. Therefore, to obtain the hysteretic characteristic on the compression side similar to that on the tension side and to mitigate pinching, it becomes necessary to avoid overall buckling (i.e., flexural buckling). The results of the first studies on overall buckling behavior of BRBs conducted by Watanabe et al. (1988) revealed that the ratio of Euler buckling load of the restraining member to the yield strength of the core, P_e/P_y, is the factor that is the most determinative for control of brace global buckling. These authors concluded that if the ratio of the Euler buckling load of the BRM to the yield load of the inner core, P_e/P_y, is less than one, the brace member will experience overall buckling during cyclic loading of the braced frame. However, a P_e/P_y ratio of 1.5 was proposed for design purposes in the studies mentioned. The criterion $P_e/P_y > 1$ has a theoretical basis (Black et al. 2002) and has been verified by Iwata et al. (2006) through experimental testing. Similar experimental studies were conducted by Usami et al. (2006) on all-steel BRBs, and a safety factor of $\gamma_f = P_{max}/P_y$ was proposed where P_{max}

and P_y denote the maximum compression force in the brace member and the core yielding capacity, respectively. The safety factor is illustrated as follows:

$$\gamma_f = \frac{1}{\frac{P_y}{P_e} + \frac{P_y}{M_y}(a + d + e)} \tag{1}$$

Where, d and e are the initial deflection, gap amplitude, and the eccentricity of loading, respectively. Test results showed that if the value of safety factor γ_f were greater than three, overall buckling of BRB would not occur. The finite element analysis method was recently used with success to predict the buckling response of the core plates in BRB members with tubes filled with mortar (Matsui et al. 2008). Subsequent finite element analysis studies have been conducted by Korrzekwa et al. (2009) to investigate the core buckling behavior in all-steel BRBs. The studies mentioned above also provided a description of the complex interaction that develops between the brace core and BRM. Outward forces induced by the contact forces were found to be resisted in flexure by the BRM components and in the bolts holding together the BRM components located on each side of the core. In addition, the contact forces resulted in longitudinal frictional forces that induced axial compression loads in the BRM. The representative P_e/P_y ratio used in these studies was 3.5, and the test results showed that the encasing strength was adequate to prevent global buckling of the brace. This paper investigates the finite element analysis studies of overall buckling behavior of all-steel BRBs regarding the effect of the gap amplitude between core and BRM and the initial imperfection of an entire BRB member. Finally, the overall buckling prevention condition of the proposed BRBs is suggested for design purposes.

2. OVERALL BUCKLING CRITERION OF BRBs

An analysis of elastic buckling of a composite brace composed of a steel core encased by a restrainer showed that the critical load of the entire brace member under compression could be found by solving an equilibrium equation as follows (Fujimoto et al. 1988):

$$E_B I_B \frac{d^2 v}{dx^2} + (v + v_0) N_{max} = 0 \tag{2}$$

in which $E_B I_B$ is the flexural stiffness of the BRM, N_y represents the brace yielding load, and v and v_0 denote the transverse and the initial deflection of the brace member, respectively, as shown in Fig. 2. The initial deflection of the brace is assumed to be expressed by a sinusoidal curve as follows:

$$v_0 = a \sin\frac{\pi x}{L} \tag{3}$$

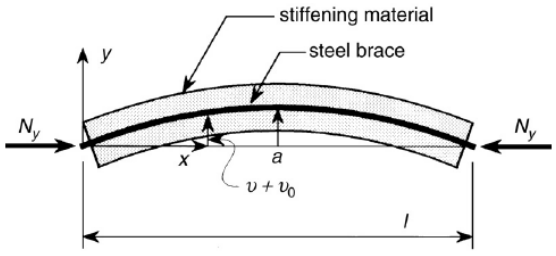

Figure 2. Force and deformation of a BRB

where a is the initial deflection of the brace at center, and N is the brace axial load, which is replaced with P in the following equations. Solving the equilibrium Eq. (2) results in the following:

$$v + v_0 = \frac{a}{1 - {P_{max}}/{P_e}} sin\frac{\pi x}{L} \quad (4)$$

The bending moment at the center of BRM can be written as follows:

$$M_C = \frac{P_{max} \, . a}{1 - {P_{max}}/{P_e}} \quad (5)$$

where P_{max} is the maximum axial force of the brace. Assuming that P_{max} is equal to the P_y (i.e., yield load of the core) and considering that the buckling of the BRB occurs when the maximum stress in the outermost fiber of the BRM reaches the yield stress, the requirement for stiffness and strength of the steel tube (BRM) can be obtained as follows:

$$\frac{P_e}{P_y} > 1 + \frac{\pi^2 E_B \, a \, D}{2\sigma_y {L_B}^2} \quad (6)$$

in which L_B , σ_y, and D denote the length, the yield stress of the steel tube, and the depth of the restraining member section, respectively. This is the first formula that successfully expresses strength and stiffness requirements as paired in the design of BRBs. In this formula, the effect of gap amplitude, g, has not been considered in the calculation of the moment at the center of the BRM. Therefore, in this paper, this parameter is involved in Eq. (6). Thus, Eq. (6) can be modified as follows:

$$\frac{P_e}{P_y} > 1 + \frac{\pi^2 E_B \, (a + g) D}{2\sigma_y {L_B}^2} \, = \beta \quad (7)$$

where L_B is the length of the core and BRM (equal together), and D is the depth of the BRM section. This equation indicates that overall buckling of the brace will not occur if the ratio P_e/P_y is greater than the parameter β, which is calculated based on the geometric and material characteristics of the brace member.

3. FINITE ELEMENT ANALYSIS

To provide a numerical understanding of the cyclic behavior and buckling load of all-steel BRBs, an analysis using the finite element analysis method was conducted on 13 BRB specimens. A tri-dimensional representation of the brace specimens was developed to properly capture the observed behavior. The models included the core plates, and the BRM components consist of tubes, guide plates, filler plates, and end stiffeners.

3.1 Description of the models

Numerical studies have been conducted on 13 proposed all-steel BRBs. Table 1 represents the details and specifications of the models where the first column shows the specimen code in the form $S_i g_i$, in which indexes i and g represent the model number and gap amplitude at the interface, respectively. All models consisted of a constant 10X1 cm^2 core plate with various cross sections for BRM members, as shown in Table 1. Therefore, the yield strength of the core was kept constant when the stiffness and strength of the BRMs were altered. In addition, the effect of the generation of a gap between the core and the BRM was considered in the analysis. The total length of the BRBs, L, was assumed to be 200 cm. The core plate's yield load, P_y, was calculated by multiplying the yield stress by the cross-sectional area, and the buckling load of the BRM, P_e, was calculated from the Euler buckling load formula.

The core plate and BRM were modeled using 8-node C3D8 brick elements. Large displacement static cyclic analysis was performed using the ABAQUS 6.9.3 general-purpose finite element program. The core plate was expected to undergo large plastic deformations and higher mode buckling with pronounced curvature. Therefore, a refined mesh was adopted with five elements across the plate and two over the thickness. A coarser mesh was used for the BRM because most of this component was expected to remain elastic. Contact properties with hard stiffness in the transverse direction and tangential coulomb frictional behavior were assumed between the core and the BRM elements. Regarding studies in the field (Chou et al. 2010), a friction coefficient of 0.1 was adopted to provide a greasy interface between the core and the BRM. The contact model allowed for the separation of the core plate from the BRM element, which enabled the higher mode buckling of the core plate. The core plate and the BRM components were made of steel with a yield stress of F_y=3700 kg/cm^2 . A young module of 2x10^6 kg/cm^2 and a poison ratio of 0.3 were assumed for the core plate and the BRM components. A nonlinear combined isotropic-kinematic hardening rule was employed to reproduce the inelastic material property and therefore an accurate cyclic behavior. The selection of the hardening parameters was based on Coupon test results, as observed in experiments conducted by Tremblay et al. (2006). In addition, the initial kinematic hardening modulus C and the rate factor γ were assumed to be 8x10^4 kg/m^2 and 75, respectively. For isotropic hardening, a maximum change in yield stress of Q_∞=1100 kg/m^2 and a rate factor of $b = 4$ were adopted. An initial imperfection of 0.2 cm (i.e., $L/1000$) was considered in both the core plate and the BRM.

Three types of interfaces between the core plate and BRM were considered in the models. In the first case, a direct contact of the core plate with the BRM was implemented, and in the second and third cases, gap amplitudes of 0.5 and 2 mm, respectively, were provided through the core thickness. In addition, Constant Gap amplitude of 2 mm was provided through the core width in all models. Such a gap was used to accommodate the free expansion of the inner core under axial loads. The axial deformation was blocked at one end of bracing with a pinned connection. Axial displacements were imposed at the other end following the cyclic quasi static protocol suggested by AISC seismic provisions for BRBs as follows: 2 cycles at $\pm\Delta_y$, 2 cycles at $\pm 0.5\Delta_{bm}$, 2 cycles at $\pm\Delta_{bm}$, 2 cycles at $\pm 1.5\Delta_{bm}$, and 2 cycles at $\pm 2\Delta_{bm}$, where Δ_y is the displacement that corresponds to the yielding of the core, and Δ_{bm} is the axial deformation of the brace corresponding to the design story drift. Based on the previous studies by Tremblay et al. (2006), the peak strain amplitude in full-length core braces typically falls in the range of 0.01 to 0.02 for common structural applications, and peak deformation in the majority of past test programs have been limited to that range (Watanabe et al. 1988). In this study, Δ_{bm} was set to 2 cm, which corresponds to the axial strain of 1% in the core, and the core yielding displacement, Δ_y, was calculated as 0.37 cm based on the material characteristics. Therefore, the ultimate axial displacement demand of the brace during cyclic loading will be $2 \times \Delta_{bm} = 4\ cm$, which corresponds to a core strain of 2%. Therefore, the adopted value for the peak strain demand of the inner core seems reasonable. A typical cross section of the proposed BRB member and its finite element representation are shown in Figs. 3 and 4, respectively.

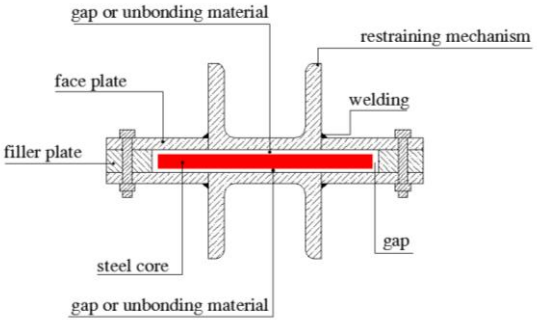

Figure 3. Typical cross section of proposed BRBs

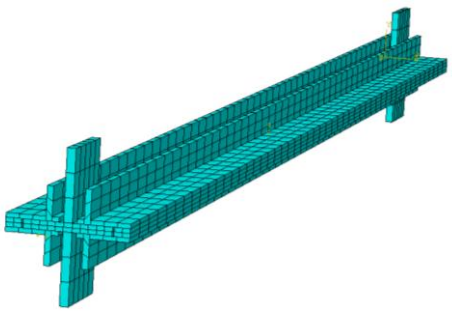

Figure 4. Finite element model of a proposed BRB

Table 1. BRB specimen properties

No.	Model name	BRM section	Core dimensions (cm)	A_c (cm^2)	gap(cm)	I_r(cm^4)	P_e(kg)	P_{yc} (kg)
1	$S_1g_{0.5}$	UNP 50 + 2 Face plate (4.5×0.5)[1]	Plate 10×1	10	0.05	85	41946	37000
2	$S_2g_{0.5}$	UNP 65 + 2 Face plate (3.75×0.5)	Plate 10×1	10	0.05	116	57165	37000
3	$S_3g_{0.5}$	BOX (5×5×0.3) + 2 Face plate (4.5×0.5)	Plate 10×1	10	0.05	153	75290	37000
4	$S_4g_{0.5}$	BOX (5×5×0.4) + 2 Face plate (4.5×0.5)	Plate 10×1	10	0.05	195	96317	37000
5	S_1g_2	UNP 50 + 2 Face plate (4.5×0.5)	Plate 10×1	10	0.2	96	47552	37000
6	S_2g_2	UNP 65 + 2 Face plate (3.75×0.5)	Plate 10×1	10	0.2	130	63950	37000
7	S_3g_2	BOX (5×5×0.3) + 2 Face plate (4.5×0.5)	Plate 10×1	10	0.2	166	81676	37000
8	S_4g_2	BOX (5×5×0.4) + 2 Face plate (4.5×0.5)	Plate 10×1	10	0.2	211	104292	37000
9	S_5g_2	PL (3.5×1) + 2 Face plate (4.5×0.5)	Plate 10×1	10	0.2	82	40697	37000
10	S_1g_0	UNP 50 + 2 Face plate (4.5×0.5)	Plate 10×1	10	0.0	81	40199	37000
11	S_2g_0	UNP 65 + 2 Face plate (3.75×0.5)	Plate 10×1	10	0.0	112	55191	37000
12	S_3g_0	BOX (5×5×0.3) + 2 Face plate (4.5×0.5)	Plate 10×1	10	0.0	148	73262	37000
13	S_4g_0	BOX (5×5×0.4) + 2 Face plate (4.5×0.5)	Plate 10×1	10	0.0	190	93761	37000

1-Dimensions in cm

4. RESULTS AND DISCUSSIONS

Hysteretic responses in all of the BRB models are well predicted by the finite element model in both elastic and nonlinear ranges. Fig. 5 illustrates the normalized hysteretic responses of the braces. Axial force-displacement curves of the BRB models are captured from a point at the brace end. This point is located in a region that essentially remains elastic because stiffener plates are provided in this region to prevent local buckling in the brace end. Therefore, the captured force-displacement relation may not be a representation of the true stress distribution of the core during cyclic loading, although the curves properly describe the deterioration in strength caused by the global or local buckling of the brace. The axial force-deformation curves shown in Fig. 5 indicates the sudden deterioration in the strength and overall buckling in the models $S_1g_{0.5}$, S_5g_2, and S_1g_0, whereas in all of the other models, stable hysteretic response without significant change in brace load carrying capacity is specified. Of course, some local decline in the hysteretic curve of the models including gap is captured because of the local buckling of the core plate under compression. The values of P_e/P_y have been calculated for all 13 BRB specimens and are given in Table 2. In addition, the factor β is calculated and shown in Table 2. Based on the results of analysis, as shown in Table 2, models with a P_e/P_y ratio greater than 1.2 do not experience overall buckling during axial loading up to a core strain of 2%. In addition, as shown in Table 2, these models experience a P_e/P_y ratio greater than β. Therefore, the analysis results confirm the validity of Eq. (7). In models S_1g_0 through S_4g_0, with direct contact of the core and the BRM, local buckling of the core plate does not occur under incremental compression loading. Fig. 5 confirms this phenomenon. In addition, Fig. 5 shows that the local declines in hysteretic curves increase because of the increase in gap amplitude. In model S_1g_0 with a P_e/P_y ratio less than 1.2, the brace member causes the lateral deflection as the compressive displacement increases and the lateral deflection rises. Contact forces acting on the upper side of the BRM increase and buckling of the brace member occurs when the moment at the center of the BRM as a result of the contact forces reaches the yield moment of the BRM. In models $S_1g_{0.5}$ and S_5g_2 with a P_e/P_y ratio smaller than 1.2, the lateral deflection rises to the deformation of the higher order buckling modes. The contact forces acting on both sides of the restraining member increase under compression and cause global buckling of the brace. The results showed that the models with a P_e/P_y ratio greater than 1.2 do not experience global buckling, regardless of the size of gap in the model. However, in the models with gaps, when P_e/P_y is greater than 1.2, severe inelastic excursions occur in the core plate under compression, which induces the lateral opening of the BRM member without overall buckling.

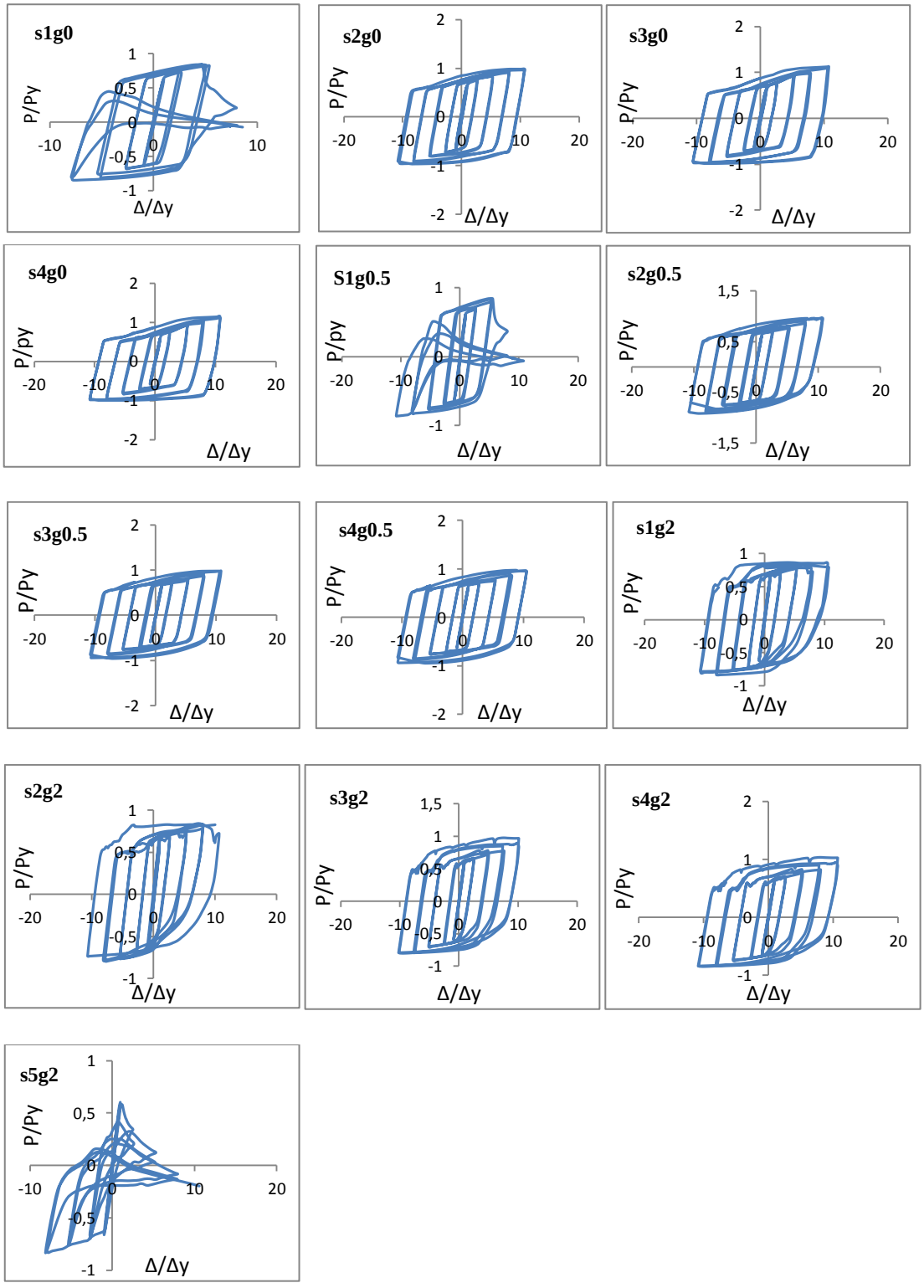

Figure 5. Hysteretic responses of the proposed BRBs

Previous studies conducted by Korrzekwa et al. (2009) also confirm this phenomenon. Therefore, providing sufficient gap between the core plate and the BRM to accommodate lateral expansion of the core plate does not significantly affect the hysteretic response of the BRB if the BRM has enough rigidity, i.e., if $P_e/P_y > 1.2$. In addition, the gap allows for free axial deformation of the core plate and reduces the amount of frictional forces at the interface. The results showed that the number of contact points between the BRM and the core plate gradually increases with more pronounced curvature. The

buckles at large compression displacements are also more closely spaced at the core ends, as shown in Fig. 6b. The opening of the BRM attributable to higher order buckling of the core in models with adequate strength of BRM is shown in Fig. 6a, indicating that the core imposes outward forces on the BRM that are resisted by the welds connecting the two upper and lower BRM components.

Table 2. Analysis results for the proposed BRBs

ABAQUS Results				
gap= 0 (Direct contact)				
Model	$\alpha = P_e/P_y$	β (Fujimoto)	Brace Global Buckling	Core Local Buckling
S1g0	1.10	1.11	Yes	No
S2g0	1.49	1.13	No	No
S3g0	1.98	1.15	No	No
S4g0	2.53	1.15	No	No
gap=0.2 cm				
S1g2	1.29	1.24	No	Yes, Opening of BRM
S2g2	1.73	1.26	No	Yes, Opening of BRM
S3g2	2.21	1.30	No	Yes, Opening of BRM
S4g2	2.82	1.30	No	Yes, Opening of BRM
S5g2	1.10	1.25	Yes	Yes
gap=0.05 cm				
S1g0.5	1.13	1.15	Yes	Yes
S2g0.5	1.54	1.16	No	Yes, Opening of BRM
S3g0.5	2.03	1.19	No	Yes, Opening of BRM
S4g0.5	2.60	1.19	No	Yes, Opening of BRM

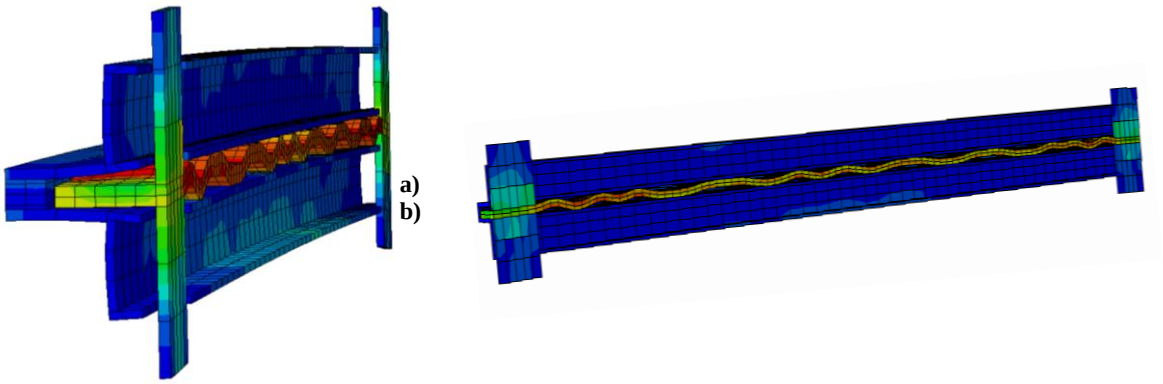

Figure 6. a) Opening of the BRM in model S_4g_2; b) Local buckling of the core in model S_1g_0

Based on the results, the authors suggest an overall buckling prevention condition of BRBs where the suggested expression is $P_e/P_y > 1.2$. The results showed that the axial force and longitudinal stress at the midpoint of the core plates in the models that buckle in compression is nearly $1.2P_y$ at the onset of the brace global buckling. If the value of the P_y in the P_e/P_y ratio is substituted by $1.2P_y$, the use of the modified equation $P_e/(1.2P_y) > 1$ or $P_e/P_y > 1.2$ instead of the original equation $P_e/P_y > 1$, proposed by Watanabe et al. (1988 and 2003), would be vindicated, and the results confirm its validity. However, a resistance factor of 0.85 may be included in the numerator for design purposes. Then, the above expression can be written as $P_e/P_y > 1.4$, which nearly coincides with the equation suggested by Powell (2005), i.e., $P_e/P_y > 1.5$.

5. CONCLUSIONS

One of the key requirements of buckling restrained braces is the performance of avoiding overall buckling until the brace member reaches target displacement and sufficient ductility. This required performance becomes important as the BRB is lightened and the strength and rigidity of the restraining member are reduced. A new generation of BRBs, called all-steel BRBs, is a class of BRBs with lighter buckling restraining components than conventional BRBs. In this family of BRBs, a light steel component is used as a restraining member instead of the mortar-filled tubes used in conventional BRBs, which may result in overall buckling of the brace caused by inadequate rigidity and strength of the restraining components. In this paper, the overall buckling prevention condition of all-steel BRBs is numerically examined by the finite element analysis method. Among the 13 BRB models, three models that had a P_e/P_y ratio of less than 1.2 experienced global buckling during cyclic loading of the brace up to a core strain of 2%. In the buckled models mentioned previously, the P_e/P_y ratio was less than factor β in Eq. (7), which confirms the validity of that equation, whereas in the other models, with a P_e/P_y ratio greater than 1.2, no buckling was captured in compression. Therefore, the authors propose an overall buckling prevention condition of $P_e/P_y > 1.2$ instead of the original equation suggested by Watanabe et al. (1988 and 2003). However, this minimum P_e/P_y ratio is thought to be applied by exerting a safety factor of 0.85. Thus, a ratio of $P_e/P_y > 1.4$ might be used for design purposes. In addition, results showed that providing a gap between the core and the BRM, despite some local instability attributable to higher mode buckling of the core, would not significantly affect the hysteretic behavior of the brace, if the strength and rigidity of the BRM are sufficient, i.e., $P_e/P_y > 1.2$.

REFERENCES

Black, C.J., Makris, N., and Aiken, I.D. (2002). Component Testing, Stability Analysis and Characterization of Buckling Restrained Braced Braces. *Report No. PEER 2002/08*, Univ. of California, Berkeley, CA

Inoue, K., Sawaizumi S., Higashibata, Y., and Inoue, K. (2001).Stiffening requirements for unbonded braces encased in concrete panels. *ASCE J. Struct. Eng*., **127(6)**: 712–719

Qiang X. (2005). State of the art of buckling-restrained braces in Asia. *Journal of Constructional Steel Research*. **61**:727-48.

Clark P., Aiken I., Kasai K., Ko E., Kimura I. (1999). Design procedures for buildings incorporating hysteretic damping devices. In: *Proc., 69th annual convention*. *SEAOC*. p. 355-71.

Sabelli R., Mahin S., Chang C. (2003). Seismic demands on steel braced frame buildings with buckling-restrained braces. *Engineering Structures*.**5**:655-66.

Fahnestock LA., Sause R., Ricles JM. (2007). Seismic response and performance of buckling-restrained braced frames. *Journal of the Structural Engineering*.**133 (9)**:1195-204.

Takeuchi T, Suzuki K, Marukawa T., Kimura Y., Ogawa T., Sugiyama T. et al. (2005). Performance of compressive tube members with buckling restrained composed of mortar in-filled steel tube. *Journal of Structure and Construction Engineering*.**590**:71-8. [In Japanese].

Tembata H., Koetaka Y., Inoue K. (2004). Out-of-plane buckling load of buckling restrained braces including brace joints. *Journal of Structure and Construction Engineering*. **581**:127-34. [In Japanese].

Kinoshita T., Koetaka Y., Inoue K., Iitani K. (2007). Criteria of buckling-restrained braces to prevent out-of-plane buckling. *Journal of Structure and Construction Engineering*. **621**:141-8. [in Japanese].

Tremblay, R., Bolduc, P., Neville, R., and DeVall, R. (2006). Seismic testing and performance of buckling restrained bracing systems. *Can. J. Civ. Eng*. **33(1)**: 183-198.

Black C., Makris N., Aiken I., (2002). Component testing, stability analysis and characterization of buckling restrained braces. *PEER Report 2002/08*, University of California at Berkeley.

Iwata, M. and Murai M. (2006). Buckling-restrained Brace Using Steel Mortar Planks; Performance Evaluationas a Hysteretic Damper. *Earthquake Engineering and Structural Dynamics*. **35**: 1807-1826.

Kato, M., Usami, T. and Kasai, A. (2002). A numerical study on cyclic elasto-plastic behavior of buckling-restraining brace members. *JSCE J. Struct. Eng*. **48A**, 641-648.

Watanabe, N., Kato, M., Usami, T. and Kasai, A. (2003). Experimental study on cyclic elasto-plastic behavior of buckling-restraining braces. *JSCE J. Earthquake Eng*. **27**, Paper No.133.

Usami, T. et al. (2006). Guidelines for Seismic and Damage Control Design of Steel Bridges, Edited by Japan Society of Steel Construction (JSSC), Gihodo-Shuppan.

Eryasar,.M. , Topkaya, C. (2010). An experimental study on steel-encased buckling restrained brace hysteretic damper, *J. of Earthquake engineering and structural dynamics*. **39**: 561-581.

AISC (American Institute of Steel Construction), Seismic provisions for structural steel buildings, Chicago, IL, 2005.

Watanabe A, Hitomi Y., Yaeki E., Wada A., Fujimoto M. (1988). Properties of braces encased in buckling-restraining concrete and steel tube. In: *Proceedings of 9th world conference on earthquake engineering*: p. 719-24.

Matsui, R., Takeuchi, T., Hajjar, J.F., Nishimoto, K., and Aiken, I.(2008). Local Buckling Restraint Condition for Core Plates in Buckling-Restrained Braces. *Proc. 14th World Conf. on Earthquake Eng*., Beijing, China, Paper No.05-05-0055.

Korrzekwa A., Tremblay, R. (2009). Numerical simulation of the cyclic inelastic behavior of buckling restrained braces, *Taylor & Francis Group*, London, ISBN 978-0-415-56326-0.

Fujimoto M,Wada A, Saeki E,Watanabe A, Hitomi Y. (1988). A study on the unbonded brace encased in buckling restraining concrete and steel tube. *Journal of Structural and Construction Engineering*, AIJ;**34B**: 249–58 [in Japanese].

ABAQUS. Standard user's manual version 6.3. Pawtucket, RI: Hibbitt, Karlsson & Sorensen, Inc.; 2003.

Chou, C., Chen, S. (2010). Subassemblage tests and finite element analyses of sandwiched buckling restrained braces, *Engineering Structures*, **32:8**, 2108-2121.

Powell, S. (2002). Personal communication, *Star Seismic LLC*, Park City, UT.